Applied Catalysis B: Environmental 185 (2016) 225–232

Contents lists available at ScienceDirect

Applied Catalysis B: Environmental

journal homepage: www.elsevier.com/locate/apcatb

Effect of carbon-dots modification on the structure and photocatalytic activity of g-C_3N_4

Shun Fang, Yang Xia, Kangle Lv*, Qin Li, Jie Sun, Mei Li*

Key Laboratory of Catalysis and Materials Science of the State Ethnic Affairs Commission & Ministry of Education, South-Central University for Nationalities, Wuhan 430074, PR China

ARTICLE INFO

Article history:
Received 5 October 2015
Received in revised form
11 December 2015
Accepted 11 December 2015
Available online 14 December 2015

Keywords:
Graphitic carbon nitride
Carbon dot
Photocatalytic degradation
Rhodamine B

ABSTRACT

As a promising metal-free photocatalyst, graphitic carbon nitride (g-C_3N_4) has attracted increasing attention. However, from the viewpoint of practical application, the quantum efficiency of g-C_3N_4 needs to be further improved. In this article, carbon dots (C-dots) modified g-C_3N_4 hybrid was successfully prepared by a novel strategy using C-dots and dicyandiamide as starting materials. The photocatalyst was characterized by scanning electron microscope (SEM), transmission electron microscopy (TEM), X-ray diffraction (XRD), FT-IR, UV–Vis diffuse reflectance spectrum (DRS), X-ray photoelectron spectroscopy (XPS), powder photoluminescence (PL) and surface photovoltage spectrum (SPS). Both the photocatalytic activity of C-dots modified g-C_3N_4 was evaluated by degradation of Rhodamine B under UV irradiation and photocatalytic hydrogen production under visible irradiation. The experimental results show that C-dots modification causes the lattice distortion of g-C_3N_4. With increase in the loading amount of C-dots, the photocatalytic activity of g-C_3N_4 increase first and then decrease. g-C_3N_4 modified with 0.25 wt.% C-dots shows the highest photocatalytic activity, which is 3 times higher than pristine g-C_3N_4. C-dots act as electron-sinks, which prevent the recombination of photo-generated electron-hole pairs, enhancing the photocatalytic activity of g-C_3N_4. However, too much C-dots become recombination centers, which is detrimental to the photocatalytic activity of g-C_3N_4.

1. Introduction

Since Wang and Domen [1] reported that a polymer semiconductor on the basis of a defecteous graphitic carbon nitride (g-C_3N_4) possesses the performance of hydrogen or oxygen production from water, the study towards this promising metal-free photocatalyst has attracted increasing attention due to its high thermal and chemical stability, semiconductivity, and special optical features [2,3]. The optical band gap of this polymer semiconductor was determined to be 2.7 eV. The g-C_3N_4 photocatalyst is considered to be stable under light irradiation in water solution as well as in acid (HCl, pH 0) or base (NaOH, pH 14) solutions due to the strong covalent bonds between carbon and nitride atoms [4]. Up to now, g-C_3N_4 has been used as a photocatalyst to reduce CO_2 [5], generate hydrogen from water [3–7], selectively oxidize alcohols [8] and decompose pollutants [9,10]. However, the quantum efficiency of g-C_3N_4 is very low. It was reported that the quantum efficiency for hydrogen production is only about 1% at 420 nm, which hampers the practical applications of g-C_3N_4 [9].

To improve the photocatalytic activity of g-C_3N_4, many strategies were used such as doping [5,9], coupling with other semiconductor [10–15], modified with carbon materials [16,17], and morphology control [18]. The study of Wang et al. also showed that the photocatalytic activity of g-C_3N_4 was greatly enhanced in the presence of H_2O_2, which acts as an efficient electron scavenger [19]. Quan et al. reported the fabrication of GO/g-C_3N_4 hybrid, and they found that GO can acts a separation center and electron acceptor, lead to a remarkable improvement in the visible light photocatalytic activity of g-C_3N_4 [20]. In photocatalytic NO oxidation, Sano et al. found that the photocatalytic activity of g-C_3N_4 increased 8 times after alkaline hydrothermal treatment, which is due to the transformation of unstable domains of g-C_3N_4 to the mesoporous structure with a higher specific surface area [21]. Recently, we found that the photocatalytic activity of g-C_3N_4 was greatly improved in acidic solution such as HF and H_2SO_4 [22], and it is proposed that acidification of g-C_3N_4 results in the formation of a new surface state, which can act as a trapping site for photo-generated electrons, retarding the recombination of carriers.

* Corresponding authors. Fax: +86 27 67842752.
E-mail addresses: lvkangle@mail.scuec.edu.cn (K. Lv), limei@mail.scuec.edu.cn (M. Li).

http://dx.doi.org/10.1016/j.apcatb.2015.12.025
0926-3373/

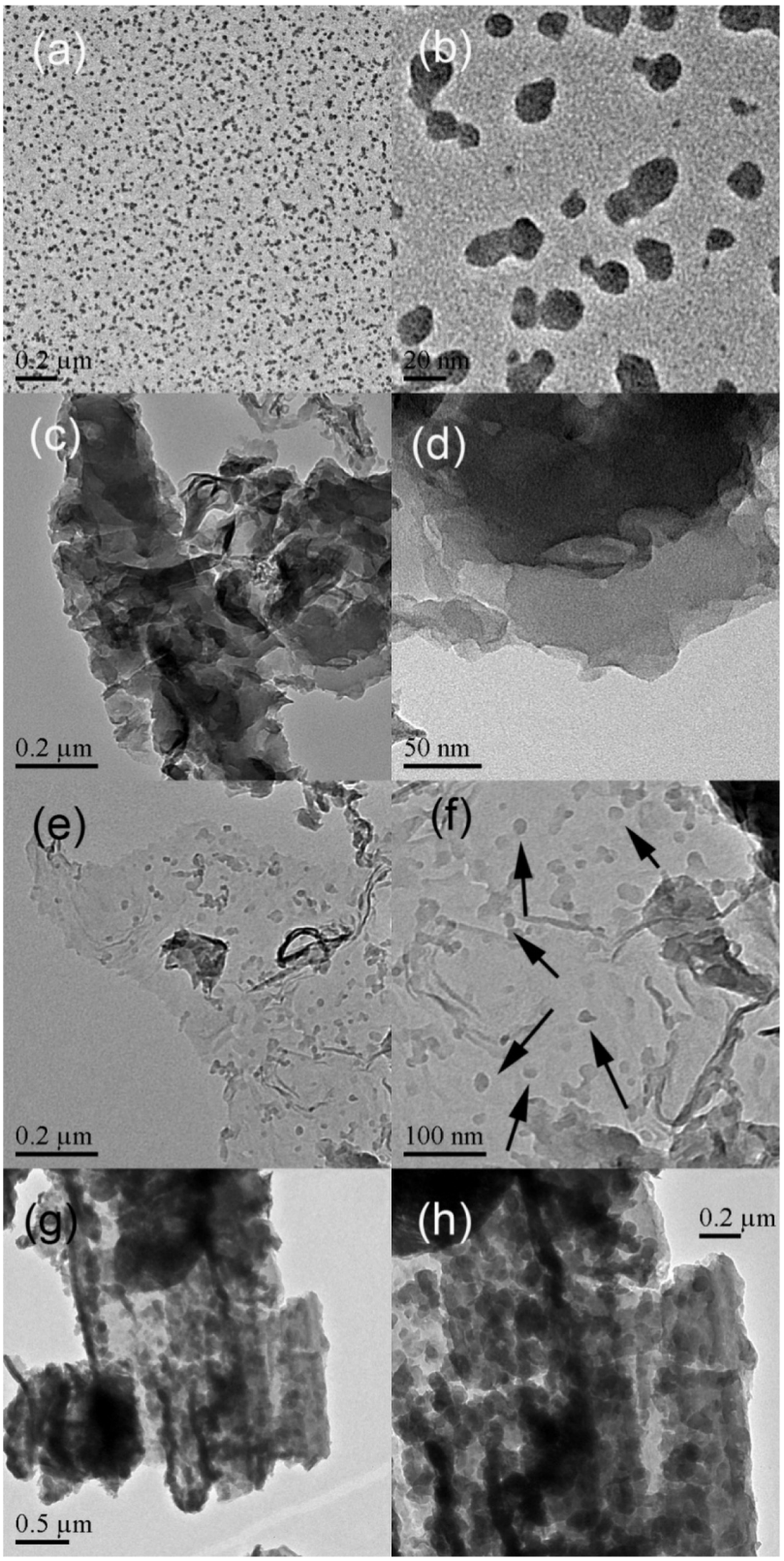

Fig. 1. TEM images of C-dots (a, b), pristine g-C_3N_4 (c, d), C-dots modified g-C_3N_4 samples of S5 (e, f) and S10 (g, h), respectively. Arrows indicate the presence of C-dots decorated on the surface of g-C_3N_4 sheets.

Very recently, Kang et al. reported the fabrication carbon nanodot modified g-C_3N_4 nanocomposite and demonstrate its impressive performance for photocatalytic solar water splitting [6]. However, the reported method in fabrication of carbon dots (C-dots) modified g-C_3N_4 hybrid is time-consuming and energy-wasting. Firstly, at least 5 days is needed for preparation of C-dots *via* an electrochemical reaction under continuous stirring. Secondly, g-C_3N_4 was prepared by calcination of urea. Lastly, C-dots

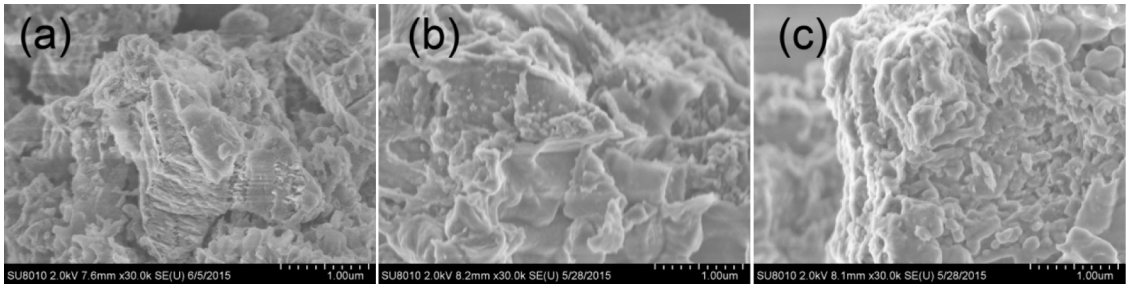

Fig. 2. SEM images of the pristine g-C_3N_4 of S0(a), C-dots modified g-C_3N_4 of S5 (b) and S10 sample (c), respectively.

modified g-C_3N_4 is prepared by mixing of C-dots with g-C_3N_4, which is followed by another calcination process. Tang et al. found that carbon quantum dot modified g-C_3N_4 showed excellent performance of near-IR (NIR) light induced H_2 evolution [23]. Similarly, the procedure for fabrication of carbon quantum dot modified g-C_3N_4 is also complex, which includes (1) pyrolysis of EDTA to fabrication of C-dots, (2) calcination of melamine to prepare bulk g-C_3N_4, (3) exfoliation of bulk g-C_3N_4 to nanosheets by thermal etching, and (4) hydrothermal reaction to prepared g-C_3N_4/C-dots hybrid.

Herein, we report a novel way for fabrication of C-dots/g-C_3N_4 hybrid by calcination of the mixture of C-dots and dicyandiamide, where C-dots was obtained from the combustion soot of an alcohol burner [24]. The effect of C-dots modification on the structure and photocatalytic activity of g-C_3N_4 was systematically studied. Compared with the work of Kang [6] and Tang [23] et al., our method for fabrication of C-dots/g-C_3N_4 hybrid is very simple.

2. Experimental section

2.1. Materials

Dicyandiamide ($C_2H_4N_4$, 99%) was obtained from Aladdin Chemical Reagent Corp., PR China. C_2H_5OH (AR) and $NH_3{\cdot}H_2O$ (AR) were purchased from Sinopharm Chemical Reagent. All other chemicals were used as received without further purification.

2.2. Preparation

C-dots were synthesized according to the literature but modifed [24]. Our approach includes: (1) collection of the soot by sitting a glass breaker upside down on top of an alcohol burner (see Fig. S1), (2) dispersing the collected soots in 50 mL of ammonia (50 v/v%) solution by ultra-sonicating for 30 min, (3) hydrothermal treatment of the suspensions in a Teflon-lined autoclave at 423 K for 7 h in an oven and (4) removal of large carbon particles from the precipitates after centrifugation at 12000 rpm for 30 min. The collected supernate containing C-dots was opened to air at room temperature removing the excess ammonia and achieving pH 7. The concentration of C-dots in stock solution was determined to be about 50 mgL^{-1} according to gravimetric analysis.

C-dots modified g-C_3N_4 was prepared similar to the fabrication of pristine g-C_3N_4. Specifically, certain amount of C-dots stock solution (0–10 mL) was added into an alumina crucible containing 10 g of dicyandiamide. The dried mixture in a crucible with cover was then heated at 823 K for 3 h. After cooled down to room temperature, the resulted yellow product was collected and milled into powder for further use. The resulted sample was labeled as "Sx", where "x" represents the volume of C-dots stock solution (mL) used for fabrication of C-dots/g-C_3N_4 hybrid (Table 1). Note that pure g-C_3N_4 sample, which was prepared in the absence of C-dots, was simply denoted as "S0".

2.3. Characterizaiton

The morphology of the photocatalyst was characterized by a transmission electron microscopy (TEM) (Tecnai G20, USA) using an acceleration voltage of 200 kV and a field emission scanning electron microscope (FESEM) (S-4800, Hitachi, Japan) with an acceleration voltage of 10 kV, respectively. The X-ray diffraction (XRD) patterns were obtained on a D8-advance X-ray diffractometer (German Bruker) using Cu Ka radiation at a scan rate of 0.02^0 $2\theta\,s^{-1}$. The accelerated voltage and applied current were 15 kV and 20 mA, respectively. FT-IR spectra were recorded on a NEXUIS-470 infrared spectrometer (Nicolet Co., U.S.A.). The UV–vis diffuse reflectance spectra (DRS) were obtained on a UV-2550 UV–vis spectrophotometer (Shimadzu, Japan). $BaSO_4$ was used as a reflectance standard in the UV–vis diffuse reflectance experiment. X-ray photoelectron spectroscopy (XPS) measurement was done using Multilab 2000 XPS system with a monochromatic Mg Kα source and a charge neutralizer, all the binding energies were referenced to the C 1s peak at 284.4 eV of the surface adventitious carbon. Photoluminescence (PL) spectra were measured at room temperature on a Fluorescence Spectrophotometer (F-7000, Hitachi, Japan). The excitation wavelength was 254 nm, the scanning speed was 1200 nm min^{-1}, and the PMT voltage was 400 V. The width of excitation slit and emission slit were both 10.0 nm. The surface photovoltage spectroscopy (SPS) measurements of the samples are carried out with a home-built apparatus [25]. The SPS signals are the potential barrier change of the testing electrode surface between that in the presence of light and that in the dark.

2.4. Evaluation of the photocatalytic activity

A 3 W LED lamp (UVEC-4 II, Shenzhen lamplic, China) emitted mainly at 365 ± 5 nm is used as light source, which is placed outside a Pyrex-glass reactor at a fixed distance (ca. 5 cm). Rhodamine B (RhB) was used as a probe molecule. During the photocatalytic reaction, the reactor was mechanically stirred at a constant rate. The concentration of C-dots modified g-C_3N_4 was 1.0 gL^{-1}, and the initial concentration of RhB was 1.0×10^{-5} mol L^{-1}. Before irradiation, the suspensions were sonicated first for 5 min, and then were shaken overnight in the dark to establish the adsorption–desorption equilibrium. At given intervals of irradiation, small aliquots were sampled and centrifuged twice at 10000 rpm for 5 min each time to remove photocatalyst nanoparticles. The concentration of RhB in supernatant was then analyzed by an Agilent 8451 spectrometer at 552 nm.

For comparison, photocatalytic degradation of RhB over C-dots modified g-C_3N_4 was also performed under visible irradiation by using two visible LED lamps emitted mainly at 420 ± 5 nm (3 W for each).

Visible photocatalytic hydrogen (H_2) production experiments were performed in a 100 mL Pyrex flask at ambient temperature and atmospheric pressure, and the openings of the flask were sealed

Table 1
Starting materials and physical properties of the pristine and C-dots modified g-C_3N_4 photocatalysts.

Sample	Starting materials		Physical properties			
	dicyandiamide (g)	C-dots (ml)[a]	XRD relative intensity[b]	PL peak intensity (a.u.)	Bandgap(eV)	Photovoltage (uV)
S0	10	0	1.00	295.1	2.72	2.07
S4	10	4	0.73	265.2	2.71	2.98
S5	10	5	0.65	251.4	2.71	3.36
S6	10	6	0.53	326.2	2.71	2.99
S10	10	10	0.45	427.5	2.72	2.61

[a] Concentration of C-dots in stock solution is 50 mg L^{-1}.
[b] XRD relative intensity of (0 0 2) peak using S0 sample as a reference.

with silicone rubber septa. A 350 W Xenon arc lamp through a UV-cutoff filter (≥420 nm), which was positioned 20 cm away from the reactor, was used as a visible-light source to trigger the photocatalytic reaction.

In a typical photocatalytic H_2-production experiment, 50 mg of the prepared photocatalyst was suspended in 80 mL of triethanolamine aqueous solution (10 v%), and then bubbled with nitrogen through the reactor for 30 min to completely remove the dissolved oxygen and ensure the reactor was in an anaerobic condition. A continuous magnetic stirrer was applied at the bottom of the reactor in order to keep the photocatalyst particles in suspension status during the whole experiments. A 0.4 mL of gas sample was intermittently sampled from the headspace of the flask through the septum, and H_2 content was analyzed by gas chromatography (GC2018, Shimadzu, Japan, TCD, with nitrogen as a carrier gas and 5A molecular sieve column).

2.5. Measurement of the formation of hydroxyl radicals

The formation of •OH radicals in solution was also performed by a photoluminescence (PL) technique using coumarin as a probe molecule, which readily reacted with •OH radicals to produce highly fluorescent product, 7-hydroxycoumarin[26]. The suspensions of the prepared g-C_3N_4 (1.0 g L^{-1}) containing coumarin (0.5 mmol L^{-1}) were mixed under magnetic stirring, and then shaken overnight. The procedure for measurement of the formation of •OH radicals under UV LED irradiation is similar to RhB degradation, except that the filtrate was analyzed on a Hitachi F-7000 fluorescence spectrophotometer by the excitation with the wavelength of 332 nm.

3. Results and discussion

3.1. Morphology

Fig. 1a and b show the TEM images of the synthesized C-dots. It can be seen that incomplete combustion of alcohol produces C-dots are relatively monodisperse, mostly in diameters of 10–20 nm. Before treatment by ammonia, these particles strongly interact with each other to form agglomerates of several micrometers (not shown here). To break down such inherent interactions and produce well dispersed, individual C-dots, we adopted an ammoniation treatment, which has been used for the purification of carbon quantum dots[6]. This method is known to introduce -NH_2 to the surfaces of C-dots, not only increasing the hydrophilicity of C-dots, but also facilitating the coupling reaction between C-dots and g-C_3N_4.

Interestingly, the color of the ammoniated C-dots changes from black to light yellow after calcination in air at 550 °C for 3 h. From the diffused reflectance spectrum, it can be seen that the absorbance of C-dots sharply decreases after calcination (Fig. S2). This is possibly due to the fact that these C-dots were oxidized to some extent during calcination in air.

The laminated structure of g-C_3N_4 is clearly shown in Fig. 1c and d. It can be seen that g-C_3N_4 is composed of highly condense two-dimensional sheets with chiffon-like ripples and wrinkles, which is stacking along the c-axis. Before modified with C-dots, the surface of g-C_3N_4 sheets is relative smooth (Fig. 1d). However, many particles with diameters of 10–20 nm are evenly decorated on the surface of g-C_3N_4 sheets (Fig. 1e and f). It has been reported that g-C_3N_4 quantum dots can be produced by chemical oxidation of g-C_3N_4 using strong oxidants [27] or acidic cutting by concentrated H_2SO_4 and HNO_3[28,29]. Therefore, these particles should be C-dots instead of g-C_3N_4 quantum dots. Fig. S3 shows a high resolution TEM image of C-dots over g-C_3N_4 (S5 sample). Although the crystallization of C-dots is weak, the lattice stripes still can be seen.

With increase in the amount of C-dots, the number of particles loaded on the surface of g-C_3N_4 increases (Fig. 1g and h for S10 sample). Element analysis showed that the element ratio of C to N for g-C_3N_4 sample steady increases from 0.651 (S0) to 0.652 (S5) and 0.654 (S10) with increase in the loading amount of C-dots, reflecting the successful modification of g-C_3N_4 by C-dots.

Fig. 2 compares the morphology of pristine and C-dots modified g-C_3N_4 samples. Unlike TEM images shown in Fig. 1, the presence of C-dots can hardly be observed from the SEM images of g-C_3N_4. This is possibly due to the fact that C-dots were covered by the stacking of g-C_3N_4 sheets.

3.2. XRD analysis

Consistent with the reports in literatures [28,30], a stronger diffraction peak at about 27° and a weaker one at about 13° were observed from the XRD pattern of pristine g-C_3N_4 (Fig. 3A) . The diffraction peak at 13° corresponds to in-plane structural packing motif of tri-s-triazine units, which is indexed as (1 0 0) peak. The distance is calculated as d = 0.67 nm. The peak at 27° corresponds to interlayer stacking of aromatic segments with distance of 0.32 nm, which is indexed as (0 0 2) peak of the stacking of the conjugated aromatic system.

With increase in the loading amount of C-dots, both the intensities of (1 0 0) and (0 0 2) diffraction peaks decrease. This reflects that the presence of C-dots prevent the polymerization of dicyandiamide and the stacking (crystallization) of g-C_3N_4 sheets. Close-up view of the (0 0 2) diffraction peak of g-C_3N_4 clearly shows the shift of the diffraction peak angle toward a lower 2θ value (Fig. 3B), which steady decreases from 27.61^0 to 27.38^0 with increase in the amount of C-dots from 0 to 10 mL. This crystal lattice distortion due to C-dots modification should result in the introduction of defects in g-C_3N_4.

3.3. FT-IR and absorption spectrum

Fig. 4 shows the FT-IR spectra of the materials prepared with different C-dots loading amount. As can be seen from Fig. 4, the vibrations at 1635 (C=N), 1574 (C=N), 1412 (C—N), 1398 (C—N),

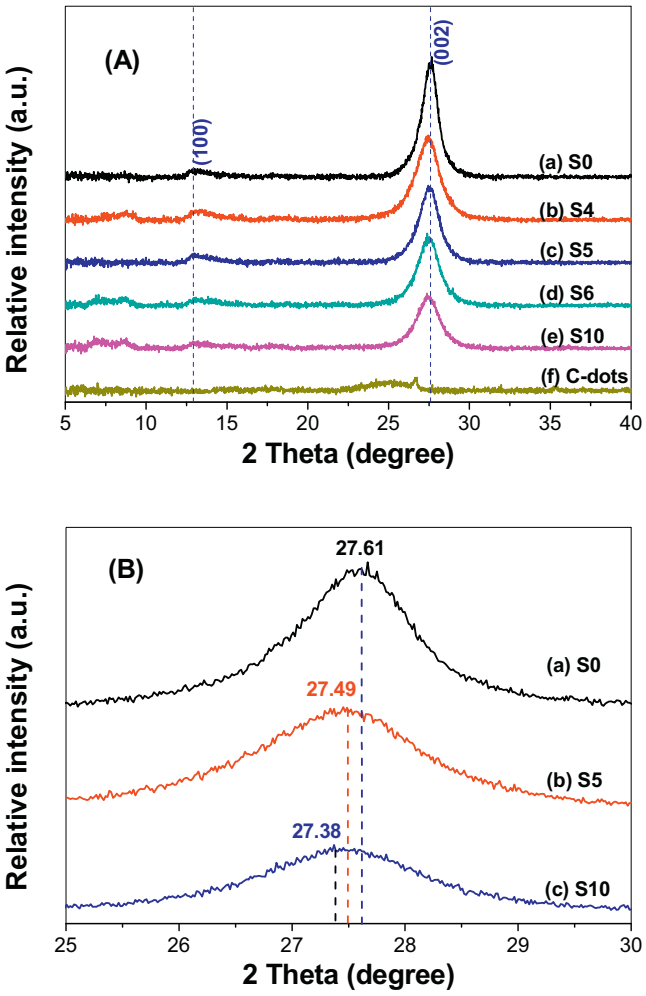

Fig. 3. XRD patterns (A) of the prepared photocatalysts (a-e) and C-dots (f), together with the enlarged part of S0, S5 and S10 sample (B), respectively.

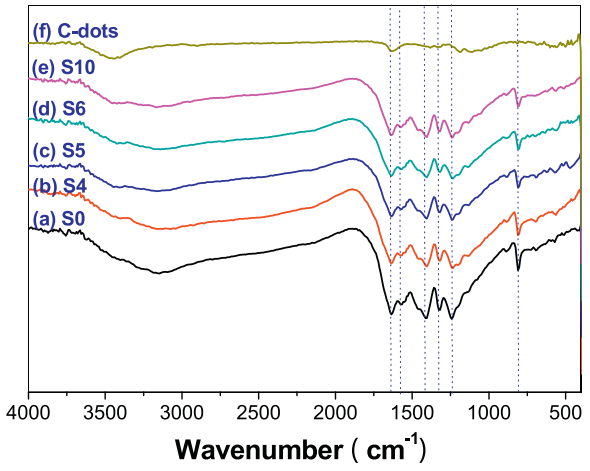

Fig. 4. FT-IR spectra of the prepared photocatalysts.

1319 (C—N) and 1242 cm^{-1} (C—N), corresponding to the typical stretching modes of CN heterocycles, and the characteristic mode of the triazine units at 810 cm^{-1}, are found for all g-C_3N_4 samples[31]. The broad bands at around 3200 cm^{-1} are indicative of stretching vibration modes for –NH of g-C_3N_4 [30].

The light harvesting ability of semiconductor is very important to its photocatalytic activity. To study the effect of C-dots

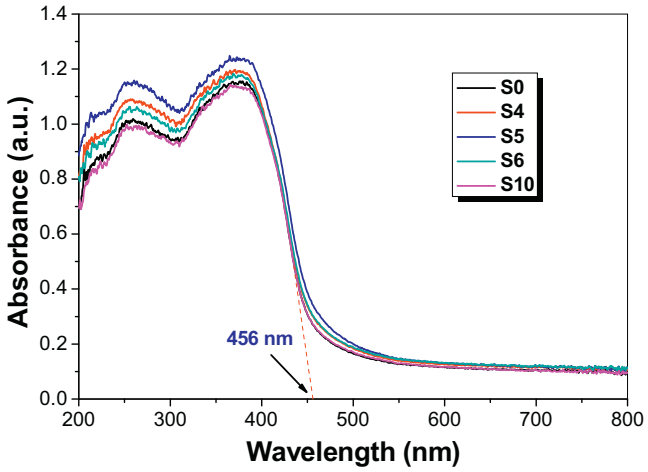

Fig. 5. UV–vis diffuse reflectance spectra of the photocatalysts.

modification on the light absorption of g-C_3N_4, the UV–vis diffuse reflectance spectra (DRS) of the photocatalysts were compared. It is found all the samples have similar light absorption spectrum (Fig. 5). Although it has been reported that the absorbance of g-C_3N_4 was enhanced in visible region after modified by C-dots[28], in our present study, C-dots show little effect on the light-harvesting ability of g-C_3N_4. This is possibly due to the fact that these C-dots are partially oxidized, which shows weak absorption in visible region (Fig. S2).

It can be seen that the onset of the absorption spectrum the pristine g-C_3N_4 begins from 456 nm, which exhibits a band gap of ca. 2.72 eV, similar to the reports in literatures[30,32]. Since all the bandgaps of the prepared g-C_3N_4 samples are similar (Table 1), the light harvesting ability should not be one of the important reasons that are responsible for the enhanced photocatalytic activity of g-C_3N_4.

3.4. XPS analysis

XPS measurements were conducted to gain insight into the chemical bonding. It was found that all the samples show similar XPS spectrum. The XPS survey spectra confirm that all the g-C_3N_4 samples are mainly composed of carbon, nitrogen, and with a small amount of oxygen (Fig. 6A) . The existence of oxygen is most likely comes from the substrate[6].

Fig. 6B and Fig. 6C show the high resolution C 1s and N1s XPS spectra for S5 sample, respectively. The C 1s spectrum can be de-convoluted into two peaks centered at 284.6 eV and 288.0 eV, respectively. The first peak is a standard carbon specialized for the sample, whereas the latter peak is a typical signal for sp2-hybridized carbon which is determined as the N— C=N backbone of the g-C_3N_4 [26,31,33]. The high resolution N 1s spectrum of S5 (Fig. 6C) reveals typical N status including pyridinic (398.5 eV), pyrrolic (400.3 eV), and graphitic (404.3 eV) N species, respectively[33]. The C 1s and N1s spectra are both similar to that of pure g-C_3N_4, which indicates the successful incorporation of C-dots on the substrate material.

3.5. Evaluation of the photocatalytic activity

Fig. 7A compares the degradation kinetics of RhB over g-C_3N_4 under UV irradiation. The degradation profiles of RhB over g-C_3N_4 can be described by the zero-order equation (Eq. (1))

$$c - c_0 = -kt \quad (1)$$

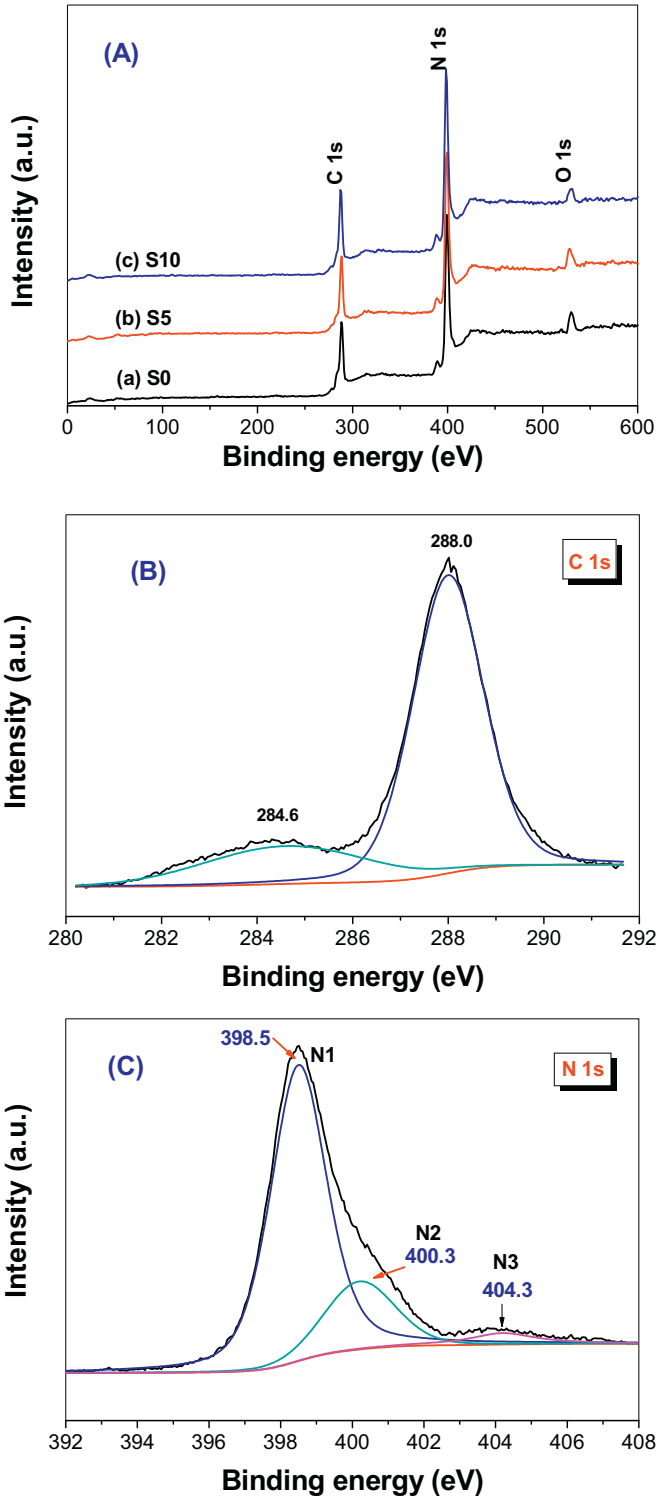

Fig. 6. XPS survey spectra of the photocatalysts (A) and the corresponding high-resolution XPS spectra of C 1s (B) and N 1s (C) of C-dots modified g-C_3N_4 (S5) sample, respectively.

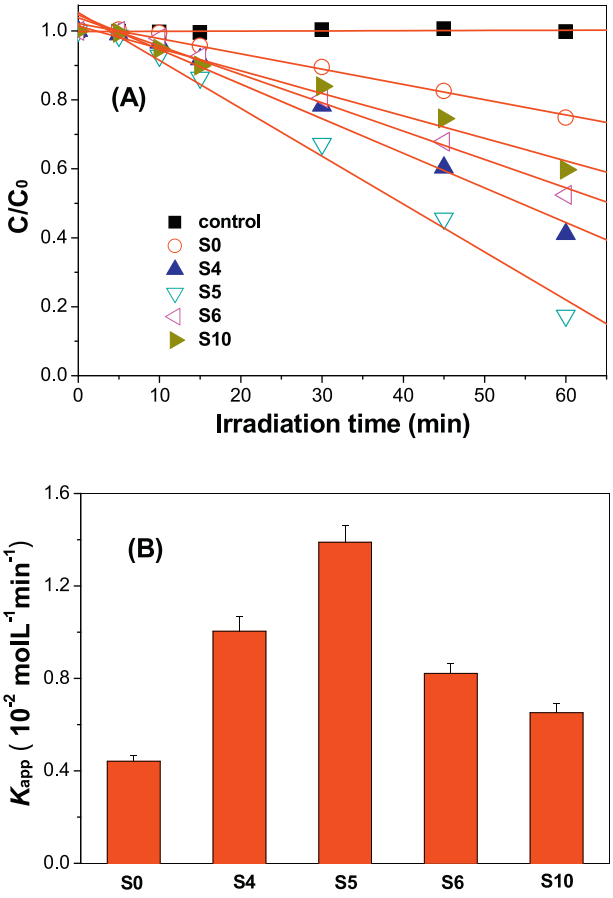

Fig. 7. Photocatalytic degradation profiles of RhB over C-dots modified g-C_3N_4 under UV irradiation (A), and the comparison of the degradation rate constant (B).

where k is the rate constant (mol L^{-1} min^{-1}), c_0 and c are initial and actual concentration of RhB dye at light irradiation time t, respectively.

Control experiment confirms that RhB is very stable, which shows little degradation under UV irradiation in the absence of g-C_3N_4 [22]. In the presence of g-C_3N_4 and UV irradiation, obvious RhB degradation can be observed. Fig. 7B compares the photocatalytic degradation rate constant of RhB over different photocatalyst. It can be clearly seen that the photocatalytic activity of g-C_3N_4 increases first and then decreases with increase in the amount of C-dots. S5 sample shows the highest photocatalytic activity (0.013 mol L^{-1} min^{-1}), which is almost 3 times higher than pristine g-C_3N_4 (0.0044 mol L^{-1} min^{-1}). Recycling experiment showed that C-dots modified g-C_3N_4 sample is very stable in degradation of RhB (Fig. S4). Similar results were also observed in degradation of RhB under visible irradiation (Fig. S5).

According to literature[34] and our previous study[22], RhB can be degraded through two different pathways: (1) hole/•OH induced formation of stepwise N-deethylated intermediates, or (2) $O_2^{\bullet-}$ radicals-induced cleavage of the whole conjugated chromophore structure. The degradation pathway of RhB can be deduced from the temporal absorption spectrum changes during photocatalytic degradation. A stepwise N-deethylation mechanism can be reflected from the marked hypsochromic shift of the spectrum. However, this hypsochromic shift is not obvious if RhB is degraded *via* cleavage of the whole conjugated chromophore structure. According to the temporal absorption spectrum changes, little hypsochromic shift can be observed for RhB degradation over pristine and C-dots modified g-C_3N_4 (Fig. S6). Therefore, it can be deduced that $O_2^{\bullet-}$ radicals are responsible for the degradation of RhB, and C-dots modification has not changed the degradation pathway of RhB over g-C_3N_4.

To further confirm the enhanced photocatalytic activity of C-dots modified g-C_3N_4, photocatalytic hydrogen production was also performed under visible irradiation. It can be seen that the hydrogen evolution rate sharply increased from 91 (S0 sample) to

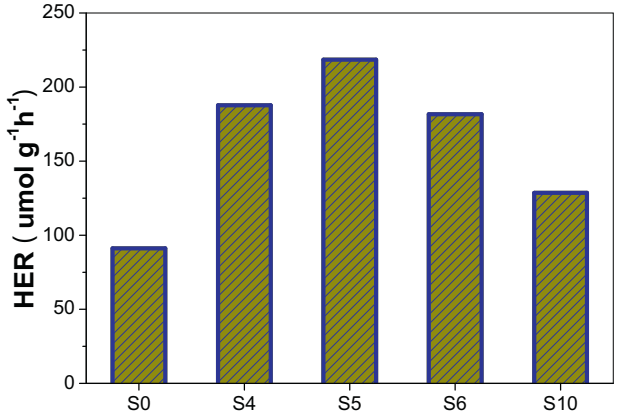

Fig. 8. Effect of C-dots modification on the photocatalytic H_2 evolution rate (HER) under visible irradiation of g-C_3N_4 photocatalyst.

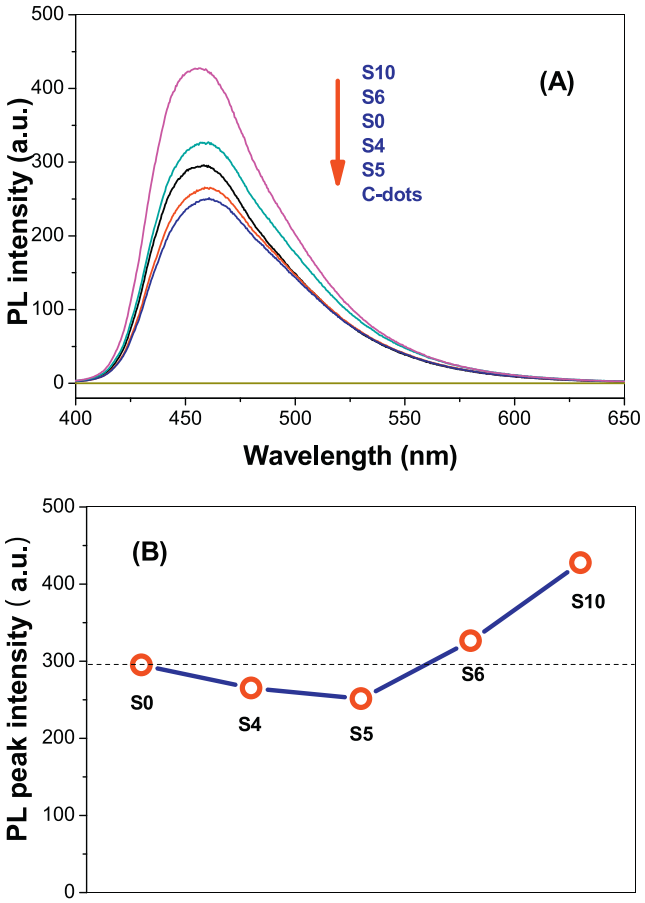

Fig. 9. PL emission spectra of the photocatalysts (A) and comparison of the corresponding PL peak intensity (B).

218 umol g^{-1} h^{-1} (S5 sample), increased by a factor of about 2.4 times (Fig. 8).

3.6. Reasons for enhanced photocatalytic activity

To account for the effect of C-dots on the enhanced photocatalytic activity of g-C_3N_4, photoluminescence (PL) analysis was performed to investigate the separation efficiency of photogenerated electrons and holes. The PL spectra of g-C_3N_4 sample before and after modified by C-dots are shown in Fig. 9A . It can be seen that the emission peaks center at 456–568 nm, which is in

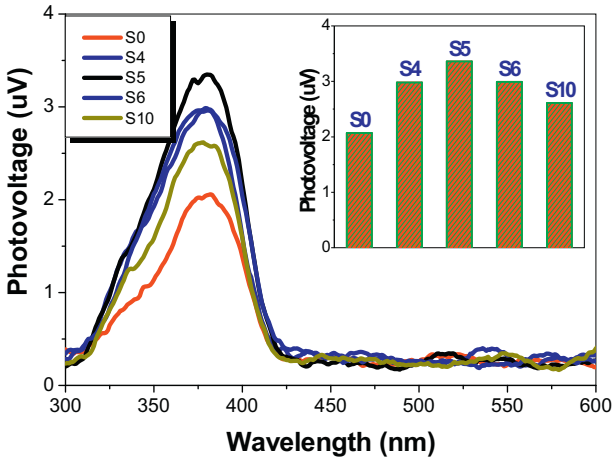

Fig. 10. SPS responses of g-C_3N_4 samples and the comparison of SPS peak intensity (inset).

accordance with the band gap of g-C_3N_4 [13,35]. This strong peak is attributed to the band–band PL phenomenon with the energy of light approximately equal to the band-gap energy of pristine g-C_3N_4.

Fig. 9B shows the dependence of PL intensity of g-C_3N_4 on the loading amount of C-dots. It can be clearly seen that the PL intensity decreases first and then increases, and S5 sample shows the lowest PL intensity. This demonstrates that the recombination of photo-generated electrons and holes is inhibited after loading small amount of C-dots, indicating that the separation of photo-generated electrons and holes in C-dots/g-C_3N_4 hybrid is more efficient than in pure g-C_3N_4. So, it is understandable that C-dots/g-C_3N_4 hybrid (S5 sample) shows superior photocatalytic activity than pure g-C_3N_4 (Fig. 7 and Fig. 8).

It has been reported that carbon materials such as graphene and carbon nanotubes can efficiently transfer photo-generated electrons from other semiconductors[36,37]. To account for the positive effect of C-dots on the enhanced photocatalytic activity of g-C_3N_4, we conducted the surface SPS signals of all the photocatalysts for reflecting the charge separation and recombination (Fig. 10). One can note that an obvious SPS response appears below 450 nm for all samples. This is attributed to the electronic transitions from the valence band (VB) to the conduction band (CB). According to the PL spectra, C-dots facilitates the electron transfer from CB of g-C_3N_4 to oxygen, retarding the recombination. Noticeably, the SPS response of g-C_3N_4 increases first and then decreases with increasing the amount of C-dots, S5 sample exhibits the highest SPS response (3.36 uV). This is well consistent with the results of PL spectra (Fig. 9). Thus, it is safe to conclude that C-dots is favorable to enhancing charge separation of g-C_3N_4. However, if the concentration of C-dots is too high, the corresponding SPS response begins to go down.

In this work, we also used coumarin as a probe to capture the formed •OH radicals in UV-illuminated g-C_3N_4 suspensions, which readily reacted with •OH radical to produce highly fluorescent product, 7-hydroxycoumarin[26]. Fig. 11 shows the PL intensity at 450 nm against the irradiation time in the presence of the photocatalyst. It can be seen that the concentration of fluorescent 7-hydroxycoumarin increases with illumination time, indicating the formation of •OH radicals. After irradiation of 240 min, the relative intensity of PL intensity @ 450 nm also increases and decreases with increasing the concentration of C-dots, and S5 shows the highest •OH radicals production rate. This is well consistent with the result of RhB degradation (Fig. 7) and photocatalytic hydrogen production (Fig. 8). Please note that the valence band position of

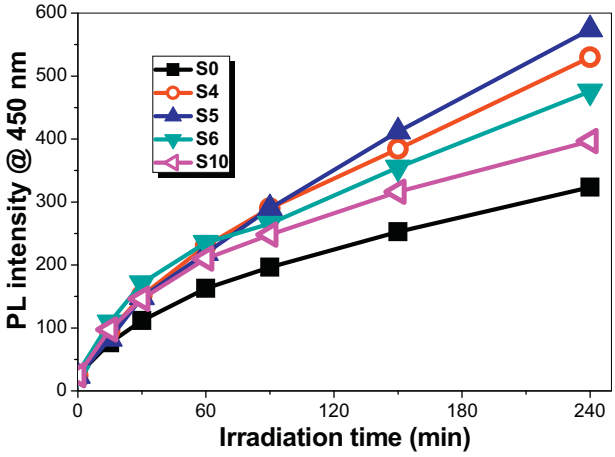

Fig. 11. Time dependence of the induced photoluminescence intensity @ 450 nm of the photocatalysts.

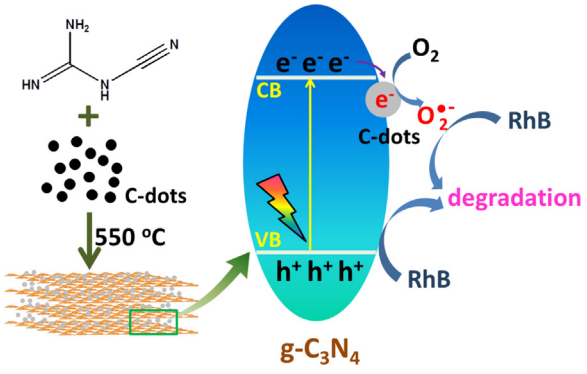

Scheme 1. Schematic diagram showing one-pot synthesis of C-dots modified g-C_3N_4 with enhanced photocatalytic activity..

g-C_3N_4 is at +1.4 V, which is not appropriate for direct generation of •OH radicals by direct hole oxidaiton (E^0(-OH/•OH) = 2.4 V) [38]. Therefore, the detected •OH radicals in solution are in fact from the CB $O_2^{\bullet-}$ radicals. This also confirms that C-dots modification can enhance the electron transfer from CB to surface adsorbed O_2, retarding the recombination of electron-hole pairs, and therefore enhancing the photocatalytic activity (Fig. 7 and Fig. 8).

The BET specific surface area of pristine g-C_3N_4 was 10.3 $m^2\,g^{-1}$ (Fig. S7). The BET areas of other C-dots modified g-C_3N_4 are measured to be 10–12 $m^2\,g^{-1}$, reflecting that C-dots has little effect on the BET specific area of g-C_3N_4. UV–vis absorption spectra have showed that the light-harvesting ability of g-C_3N_4 was not improved after modified by C-dots (Fig. 5). Therefore, the enhanced photocatalytic activity of g-C_3N_4 can be attributed to the C-dots mediated efficient electron transfer from the conduction band of g-C_3N_4 to adsorbed O_2, forming $O_2^{\bullet-}$ (Scheme 1). However, too much C-dots can act as recombination centers, reducing the photocatalytic activity of g-C_3N_4.

4. Conclusions

In summary, we reported a facile method on fabrication C-dots modified g-C_3N_4 hybrid using dicyandiamide and C-dots as starting materials. With increase in the amount of C-dots, the lattice distortion of g-C_3N_4 becomes obvious, and the photocatalytic activity of g-C_3N_4 increases first and then decreases. PL spectra and SPS characterization results indicate that C-dots can efficient transfer of photo-generated electrons from CB of g-C_3N_4 to adsorbed oxygen, retarding the recombination of electron-hole pairs. Therefore, the photocatalytic activity of g-C_3N_4 was greatly enhanced after C-dots modification. However, too much C-dots can also act as recombination centers, reducing the photoreactivity of g-C_3N_4.

Acknowledgements

This work was supported by Program for New Century Excellent Talents in University (NCET-12-0668), National Natural Science Foundation of China (21373275) and Natural Science Foundation of South-Central University for Nationalities (XTZ15016).

Appendix A. Supplementary data

Supplementary data associated with this article can be found, in the online version, at http://dx.doi.org/10.1016/j.apcatb.2015.12.025.

References

[1] X.C. Wang, K. Maeda, A. Thomas, K. Takanabe, G. Xin, J.M. Carlsson, K. Domen, M. Antonietti, Nat. Mater 8 (2009) 76.
[2] G.H. Dong, K. Zhao, L.Z. Zhang, Chem. Commun. 48 (2012) 6178.
[3] S.W. Cao, J.G. Yu, J. Phys. Chem. Lett. 5 (2014) 2101.
[4] S.W. Cao, J.X. Low, J.G. Yu, M. Jaroniec, Adv. Mater. 27 (2015) 2150.
[5] K. Wang, Q. Li, B.S. Liu, B. Cheng, W.K. Ho, J.G. Yu, Appl. Catal. B 176–177 (2015) 44.
[6] J. Liu, Y. Liu, N.Y. Liu, Y.Z. Han, X. Zhang, H. Huang, Y. Lifshitz, S.T. Lee, J. Zhong, Z.H. Kang, Science 347 (2015) 970.
[7] S.W. Cao, Y.P. Yuan, J. Barber, S.C.J. Loo, C. Xue, Appl. Surf. Sci. 319 (2014) 344.
[8] F.Z. Su, S.C. Mathew, G. Lipner, X.Z. Fu, M. Antonietti, S. Blechert, X.C. Wang, J. Am. Chem. Soc. 132 (2010) 16299.
[9] S.C. Yan, Z.S. Li, Z.G. Zou, Langmuir 26 (2010) 3894.
[10] Z.A. Huang, Q. Sun, K.L. Lv, Z.H. Zhang, M. Li, B. Li, Appl. Catal. B 164 (2015) 420.
[11] S. Kumar, T. Surendar, A. Baruah, V. Shanker, J. Mater. Chem. A 1 (2013) 5333.
[12] J.G. Yu, S.H. Wang, J.X. Low, W. Xiao, Phys. Chem. Chem. Phys. 15 (2013) 16883.
[13] S.C. Yan, S.B. Lv, Z.S. Li, Z.G. Zou, Dalton Trans. 39 (2010) 1488.
[14] K. Katsumata, R. Motoyoshi, N. Matsushita, K. Okada, J. Hazard. Mater. 260 (2013) 475.
[15] T. Li, L. Zhao, Y. He, J. Cai, M. Luo, J. Lin, Appl. Catal. B 129 (2013) 255.
[16] X.J. Bai, L. Wang, Y.J. Wang, W.Q. Yao, Y.F. Zhu, Appl. Catal. B 152–153 (2014) 262.
[17] Y. Zhao, F. Zhao, X.P. Wang, C.Y. Xu, Z.P. Zhang, G.Q. Shi, L.T. Qu, Angew. Chem. Int. Ed. 53 (2014) 13934.
[18] B.C. Zhu, P.F. Xia, W.K. Ho, J.G. Yu, Appl. Surf. Sci. 344 (2015) 188.
[19] Y.J. Cui, Z.X. Ding, P. Liu, M. Antonietti, X.Z. Fu, X.C. Wang, Phys. Chem. Chem. Phys. 14 (2012) 1455.
[20] G.Z. Liao, S. Chen, X. Quan, H.T. Yu, H.M. Zhao, J. Mater. Chem. 22 (2012) 2721.
[21] T. Sano, S. Tsutsui, K. Koike, T. Hirakawa, Y. Teramoto, N. Negishi, K. Takeuchi, J. Mater. Chem. A 1 (2013) 6489.
[22] S. Fang, K.L. Lv, Q. Li, H.P. Ye, D.Y. Du, M. Li, Appl. Surf. Sci. 358 (2015) 336.
[23] X.Y. Xia, N. Deng, G.W. Cui, J.F. Xie, X.F. Shi, Y.Q. Zhao, Q. Wang, W. Wang, B. Tang, Chem. Commun. 51 (2015) 10899.
[24] H. Liu, T. Ye, C. Mao, Angew. Chem. Int. Ed. 46 (2007) 6473.
[25] Y.B. Luan, L.Q. Jing, Y. Xie, X.J. Sun, Y.J. Feng, H.G. Fu, ACS Catal. 3 (2013) 1378.
[26] Z.Y. Wang, K.L. Lv, G.H. Wang, K.J. Deng, D.G. Tang, Appl. Catal. B 100 (2010) 378.
[27] J.H. Oh, R.J. Yoo, S.Y. Kim, Y.J. Lee, D.W. Kim, S. Park, Chem. Eur. J. 21 (2015) 6241.
[28] W.J. Wang, J.C. Yu, Z.R. Shen, D.K.L. Chan, T. Gu, Chem. Commun. 50 (2014) 10148.
[29] X.D. Zhang, H.X. Wang, H. Wang, Q. Zhang, J.F. Xie, Y.P. Tian, J. Wang, Y. Xie, Adv. Mater. 26 (2014) 4438.
[30] F. Dong, L.W. Wu, Y.J. Sun, M. Fu, Z.B. Wu, S.C. Lee, J. Mater. Chem. 21 (2011) 15171.
[31] Z.X. Zhou, J.H. Wang, J.C. Yu, Y.F. Shen, Y. Li, A.R. Liu, S.Q. Liu, Y.J. Zhang, J. Am. Chem. Soc. 137 (2015) 2179.
[32] S.C. Yan, Z.S. Li, Z.G. Zou, Langmuir 25 (2009) 10397.
[33] G.G. Zhang, S.H. Zang, X.C. Wang, ACS Catal. 5 (2015) 941.
[34] C.C. Chen, W. Zhao, P.X. Lei, J.C. Zhao, N. Serpone, Chem. Eur. J. 10 (2004) 1956.
[35] Y.G. Li, X.L. Wei, H.J. Li, R.R. Wang, J. Feng, H. Yun, A.N. Zhou, RSC Adv. 5 (2015) 14074.
[36] Y.J. Wang, R. Shi, J. Lin, Y.F. Zhu, Appl. Catal. B 100 (2010) 179.
[37] H.B. Fu, T.G. Xu, S.B. Zhu, Y.F. Zhu, Environ. Sci. Technol. 42 (2008) 8064.
[38] Y.J. Cui, J.H. Huang, X.Z. Fu, X.C. Wang, Catal. Sci. Technol. 2 (2012) 1396.